Differential regulation of auxin and cytokinin during the secondary vascular tissue regeneration in Populus trees

Chen, Jia-Jia

2019-10

Chen , J-J , Wang , L-Y , Immanen , J , Nieminen , K , Spicer , R , Helariutta , Y , Zhang , J & He , X-Q 2019 , ' Differential regulation of auxin and cytokinin during the secondary vascular tissue regeneration in Populus trees ' , New Phytologist , vol. 224 , no. 1 , pp. 188-201 . https://doi.org/10.1111/nph.16019

http://hdl.handle.net/10138/325037
https://doi.org/10.1111/nph.16019

acceptedVersion

New Phytologist

Research

Differential regulation of auxin and cytokinin during the secondary vascular tissue regeneration in *Populus* trees

Jia-Jia Chen[1,2,3]*, Ling-Yan Wang[1]*, Juha Immanen[3,4], Kaisa Nieminen[4], Rachel Spicer[5], Ykä Helariutta[2,3,6], Jing Zhang[2,3] and Xin-Qiang He[1]

[1]State Key Laboratory of Protein and Plant Gene Research, School of Life Sciences, Peking University, Beijing 100871, China; [2]Institute of Biotechnology, HiLIFE, University of Helsinki, Helsinki 00014, Finland; [3]Organismal and Evolutionary Biology Research Programme, Faculty of Biological and Environmental Sciences, Viikki Plant Science Centre, University of Helsinki, Helsinki 00014, Finland; [4]Natural Resources Institute Finland (Luke), Production Systems, Plant Genetics, Viikinkaari 1, FI-00790 Helsinki, Finland; [5]Department of Botany, Connecticut College, New London, CT 06320, USA; [6]The Sainsbury Laboratory, University of Cambridge, Bateman Street, Cambridge CB2 1LR, UK

Authors for correspondence:
Jing Zhang
Tel: +358-294159425
Email: jing.zhang@helsinki.fi

Xin-Qiang He
Tel: +86-1062757016
Email: hexq@pku.edu.cn

Received: *23 April 2019*
Accepted: *14 June 2019*

New Phytologist (2019)
doi: 10.1111/nph.16019

Key words: auxin, cambium, cytokinin, phloem, *Populus*, vascular tissue regeneration.

Summary

- Tissue regeneration upon wounding in plants highlights the developmental plasticity of plants. Previous studies have described the morphological and molecular changes of secondary vascular tissue (SVT) regeneration after large-scale bark girdling in trees. However, how phytohormones regulate SVT regeneration is still unknown.
- Here, we established a novel *in vitro* SVT regeneration system in the hybrid aspen (*Populus tremula* × *Populus tremuloides*) clone T89 to bypass the limitation of using field-grown trees. The effects of phytohormones on SVT regeneration were investigated by applying exogenous hormones and utilizing various transgenic trees. Vascular-tissue-specific markers and hormonal response factors were also examined during SVT regeneration.
- Using this *in vitro* regeneration system, we demonstrated that auxin and cytokinin differentially regulate phloem and cambium regeneration. Whereas auxin is sufficient to induce regeneration of phloem prior to continuous cambium restoration, cytokinin only promotes the formation of new phloem, not cambium. The positive role of cytokinin on phloem regeneration was further confirmed in cytokinin overexpression trees. Analysis of a DR5 reporter transgenic line further suggested that cytokinin blocks the re-establishment of auxin gradients, which is required for the cambium formation. Investigation on the auxin and cytokinin signalling genes indicated these two hormones interact to regulate SVT regeneration.
- Taken together, the *in vitro* SVT regeneration system allows us to make use of various molecular and genetic tools to investigate SVT regeneration. Our results confirmed that complementary auxin and cytokinin domains are required for phloem and cambium reconstruction.

Introduction

Plants are highly capable of repairing their damaged body parts through the regeneration strategy for survival in natural environments. More than a century ago, Gottlieb Haberlandt (1902) hypothesized the totipotency theory to explain the remarkable developmental plasticity of plants. Studies have found that various plant primary tissues from root, shoot and leaf explants are capable of regeneration under proper conditions (Xu & Huang, 2014; Nishihama *et al.*, 2015; Ikeuchi *et al.*, 2016). The secondary vascular tissues (SVTs), composed of phloem, xylem and the lateral meristem cambium between them, can also be re-established after bark strip separation in trees (Brown & Sax, 1962) or even after a large-scale bark girdling in *Eucommia* and *Populus* trees (Pang *et al.*, 2008; Zhang *et al.*, 2011). However, current studies are mainly focused on the regeneration of primary tissues, and less attention has been paid to secondary tissue regeneration. So far, it is still unclear how various regulators, including phytohormones, act in the process of SVT regeneration due to the limitation of using *in situ* systems in trees (Chen *et al.*, 2014).

Generally, *de novo* regeneration occurs in response to various external stimuli, such as wounding and grafting (Xu & Huang, 2014; Melnyk *et al.*, 2015; Chen *et al.*, 2016a; Efroni *et al.*, 2016; Iwase *et al.*, 2017). The *in situ* SVT regeneration system after large-scale bark girdling was initially established in *Eucommia* to allow repeated bark harvest for medicinal purposes (Li *et al.*, 1981) and was successfully expanded to the model tree *Populus* (Li & Cui, 1988; Cui *et al.*, 1989; Du *et al.*, 2006; Pang *et al.*, 2008; Zhang *et al.*, 2011). This *in situ* SVT regeneration system has two features: first, the phloem is restored earlier than a functional cambium; second, both phloem and cambium are derived from the remnant differentiating xylem cells (Pang *et al.*, 2008;

*These authors contributed equally to this work.

Zhang *et al.*, 2011). These findings are consistent with the discovery that, during tissue regeneration in Arabidopsis, the differentiating cells switch cell fates directly without reverting to functional stem cells (Sena *et al.*, 2009; Correa *et al.*, 2012). Therefore, elucidating the regulation of SVT regeneration would help us to understand the general mechanisms of tissue regeneration in all plants.

The involvement of the phytohormones auxin and cytokinin (CK) during plant regeneration has been demonstrated in various systems. It is well known that different CK-to-auxin ratios revealed distinct effects on organogenesis *in vitro* (Skoog & Miller, 1957; Zhao *et al.*, 2013). The roles of auxin and CK appeared versatile, depending on the regeneration systems. Generally, wounding serves as a signal leading to the accumulation of auxin, followed by sequential cellular events during regeneration in plants (Liu *et al.*, 2014; Chen *et al.*, 2016b). During adventitious root formation from Arabidopsis leaf explants, the redistribution of auxin maxima promotes cell fate transition from procambium cells to root founder cells, leading to the regeneration of root stem cell organizer (Liu *et al.*, 2014). On the other hand, elevated CK can induce the re-establishment of the shoot stem cell niche marked by *WUS* (Che *et al.*, 2007; Gordon *et al.*, 2009). CK can stimulate auxin accumulation and redistribution in calli (Kakani *et al.*, 2009), whereas increasing the CK concentration can lead to more diffuse, reduced, or even the loss of auxin maxima during root formation from explants (Pernisova *et al.*, 2009). Intriguingly, auxin is able to induce the production of CK during root organogenesis, which in turn modulates root formation (Pernisova *et al.*, 2009). It is also suggested that an antagonistic pattern of auxin and CK response signals could provide positional information for the stem cell fate decisions during shoot and root tip regeneration (Cheng *et al.*, 2013; Efroni *et al.*, 2016; Meng *et al.*, 2017). Previous reports in various systems suggest that the functions and interactions of auxin and CK during regeneration are organ or tissue specific. Therefore, it is essential to explore how these two hormones act during SVT regeneration.

Auxin and CK also play important roles during normal SVT development (Zhang *et al.*, 2014). Several decades ago, trees were discovered to have a radial gradient of auxin concentration across the SVT with a maximum located in the cambium zone (Uggla *et al.*, 1996; Bhalerao & Fischer, 2014). By contrast, the distribution pattern of CKs across the SVT in trees shows a peak in the developing phloem side, which is distinct but partially overlapping with the auxin domain (Immanen *et al.*, 2016). Tissue-specific transcriptome profiling analysis in *Populus* has shown that several auxin and CK signalling- and transport-related genes are differentially expressed during SVT regeneration, indicating that the hormone distribution is altered during this process (Zhang *et al.*, 2011). Nevertheless, how auxin and CK regulate the regeneration of a specific tissue is not clear.

The *in situ* SVT regeneration system has been very useful to study the morphological progression and molecular profiling of SVT regeneration (Li & Cui, 1988; Cui *et al.*, 1995; Du *et al.*, 2006; Pang *et al.*, 2008; Zhang *et al.*, 2011). However, it is difficult to assess how hormones affect regeneration due to the endogenous hormone sinks from the ungirdled part of the tree and the challenges associated with applying exogenous hormones in this system. Therefore, this work is aimed at developing a well-controlled *in vitro* system to study SVT regeneration, and to explore the roles of auxin and CK in this process. With a newly established *in vitro* SVT regeneration system combined with various tissue identity markers and transgenic trees, we show that auxin and CK differentially regulate phloem and cambium regeneration after bark girdling in *Populus*. Our findings additionally indicate diverse auxin–CK interactions taking place during repatterning of different vascular tissues.

Materials and Methods

Plant materials and cloning

The hybrid aspen (*Populus tremula* × *Populus tremuloides*) clone T89 was used as wild-type (WT) trees. Transgenic *Populus* trees, including *PttLMX5::AtIPT7* (Immanen *et al.*, 2016), *pBpCRE1::AtCKX2* (Nieminen *et al.*, 2008), *pAIL1:UidA* (*pAIL1:GUS*) (Karlberg *et al.*, 2011) and *PtaDR5:GUS* (Spicer *et al.*, 2013), were obtained and used in this study. The new transgenic line *PttLMX5::AtCKI1* was generated in this study. The full coding sequence of *ARABIDOPSIS CYTOKININ-INDEPENDENT 1* (*AtCKI1*, AT2G47430) was amplified with primer CKI1_cDNA_attB1_FP (5′-ggggacaagtttgtacaaaaaagcaggctggATGATGGTGAAAGTTACAAAGC-3′) and CKI1_cDNA_attB2_RP (5′-ggggaccactttgtacaagaaagctgggtaCTAGTGACGTTTGCTTTC GAT-3′) from the complementary DNA (cDNA) of Arabidopsis seedling and subsequently cloned into a Gateway entry clone vector. The final expression construct driven by LMX5 promoter (Love *et al.*, 2009) was transformed into WT clone T89 to generate transgenic trees as previously described (Immanen *et al.*, 2016). The induction levels of *AtCKI1* and *Populus RESPONSE REGULATOR 7* (*PtRR7*) were checked by quantitative reverse transcription PCR (qRT-PCR) as described subsequently to select the best line for regeneration experiments. *Populus* trees were grown for 3 months in a glasshouse under long day conditions (16 h : 8 h, light : dark) at 25°C before the girdling experiments. Transgenic trees of *pBpCRE1::AtCKX2* were grown in a glasshouse for 5 months because of their severely decreased growth (Nieminen *et al.*, 2008).

Establishment of the *in vitro* SVT regeneration platform

The split-medium was used and made as described by Agusti *et al.* (2011) with the following modifications. Standard 9 cm Petri dishes were filled with 50 ml ½ Murashige & Skoog (MS) medium containing 2.2 g l^{-1} MS (Duchefa), 30 g l^{-1} sucrose (Sigma), 10 g l^{-1} agar (Difco), 0.5 g l^{-1} MES hydrate (Duchefa). After a medium strip, 2 cm wide, was cut and removed from the centre of the plates, the volumes of the leftover medium were calculated. Corresponding volumes of the stock solutions of auxin (naphthaleneacetic acid (NAA)) were added to the media halves at fixed positions. CK (*trans*-zeatin (tZ)) was ubiquitously

applied in the medium before solidification. The plates were kept at 4°C for 1 wk to allow the hormone diffusion in the medium.

The poplar stems were collected and checked with hand-cut sections by toluidine blue O (TBO) staining under Leica 2500 light microscope. The stems were cut into 4 cm long fragments and sterilized as previously reported (Agusti *et al.*, 2011) with the following modifications. The stem fragments were surface sterilized with 70% ethanol for 45 s followed with 2% Klori (chlorine) for 15 min. Both ends of the stem fragments were excised with a sterilized razor blade. Next, the stem bark was peeled off and the girdled segments bridged vertically on the split-plate with two ends laid on apical (upper) and basal (lower) medium of the plates respectively (Fig. 1b). Samples were then incubated vertically in the growth chamber (Sanyo) under long day conditions (16 h : 8 h, light : dark) at 25°C.

Sampling and histological analysis

To examine the expression of vascular tissue identity markers, RNA samples from the sequential tangential cryo-sections crossing the SVTs as described by Nieminen *et al.* (2008) were used.

The regenerated samples were harvested at 0, 3, 6, 9 and 13 d after girdling (DAG). The regenerated tissues scraped from the surface were ground with mortars and pestles after freezing in the liquid nitrogen for further RNA extraction. For histological analysis, the middle part (*c.* 1 cm in length) of each stem fragment that did not touch the medium was sampled. The harvested stem samples were fixed with 4% paraformaldehyde and 0.2% glutaraldehyde in 0.01 M phosphate-buffered saline (pH 7.2), then embedded with LR White resin (Sigma). Thin plastic sections (5 μm) were cut with a Leica microtome and stained with TBO before imaging. Aniline blue staining was performed in hand-cut sections as described by Zhang *et al.* (2011). β-Glucuronidase (GUS) staining was carried out on hand-cut sections as described by Nieminen *et al.* (2008); ruthenium red (0.05% in water) was used as a contrast stain. For histological analysis, sections from at least 10 individual fragments were imaged for each time point within one treatment. Three to five independent experiments that were repeated produced similar results. Plastic longitudinal- or cross-sections were used to calculate the number of regenerated cambial cells (see following subsection).

Quantification of regenerated cambial cell and statistical analysis

The number of regenerated cambial cells per section was counted on the plastic longitudinal- or cross-sections (×20 magnification). First, we considered 'continuous cambium' to be where at least four uninterrupted flat cambial cells adjacent to immature xylem cells that were undergoing periclinal division was observed. All cambial cells in such a region were counted as regenerated cambial cells. In some sections from 9 DAG, the number was counted as zero when no continuous cambium was observed. A two-tailed Student's *t*-test was used to calculate the *P* value to determine the significant differences. Statistical analyses and box plots were performed using Prism (GraphPad Software, La Jolla, CA, USA, http://www.graphpad.com).

Identification of *Populus* phloem marker genes and phylogenetic analysis

The orthologues of two phloem tissue identity marker genes in Arabidopsis *ALTERED PHLOEM DEVELOPMENT* (*AtAPL*, AT1G79430) (Bonke *et al.*, 2003) and *CALLOSE SYNTHASE 7* (*AtCALS7*, AT1G06490) (Xie *et al.*, 2011) were identified with the Blastp program using the protein sequences of *AtAPL* and *AtCALS7* as baits against the *Populus* genome as described in Karlberg *et al.* (2011). The amino acid sequence alignment was performed using ClustalX2, and the neighbour-joining method was used to construct the phylogenetic trees by Mega6 with the default settings.

qRT-PCR and statistics

Total RNA was extracted using an RNeasy Plant Mini kit (Qiagen) with an on-column DNase I treatment, as described elsewhere (Immanen *et al.*, 2016). A 1 μg sample of total RNA was used to synthesize cDNA using the First Strand cDNA Synthesis Kit (Thermo Scientific) with random hexamer primer according to the manufacturer's instructions.

The diluted cDNA (1 : 6) was used as the template for the qRT-PCR reaction, and four technical repeats were done for each reaction. All qRT-PCR reactions were performed on a LightCycler 480 (Roche) with LightCycler 480 SYBR Green I master mix (Roche) and the manufacturer's qRT-PCR program. *Populus UBIQUITIN-LIKE* (*PtUBQ*) was used as the reference gene unless stated otherwise. The relative expression level for each sample was normalized to the sample collected at 0 DAG in each experiment and calculated using the comparative C_T ($\Delta\Delta C_T$) method (Livak & Schmittgen, 2001). Data obtained from three independent biological replicates were used for statistical analysis. Pairwise comparison was carried out for each hormone-treated sample against the control sample (without any hormone) at the same stage (DAG) using a two-tailed Student's *t*-test. All statistical analyses were performed using Spss software (SPSS Inc., Chicago, IL, USA). The sequences of all primers used for qRT-PCR are listed in Supporting Information Table S1. The exact *P* value for each comparison is listed in the Table S2.

Results

Auxin induces both phloem and cambium restoration during *in vitro* SVT regeneration

Here, we first established an *in vitro* SVT regeneration system in the hybrid *Populus* WT trees (T89; Fig. 1a). Stem fragments were taken from actively growing trees and cultured on the split-medium containing exogenous auxin (NAA) after bark girdling (Fig. 1b). Before girdling, a typical SVT radial pattern was displayed and the phloem-specific callose deposition was detected with aniline blue staining (Fig. 1c). Upon girdling,

New Phytologist

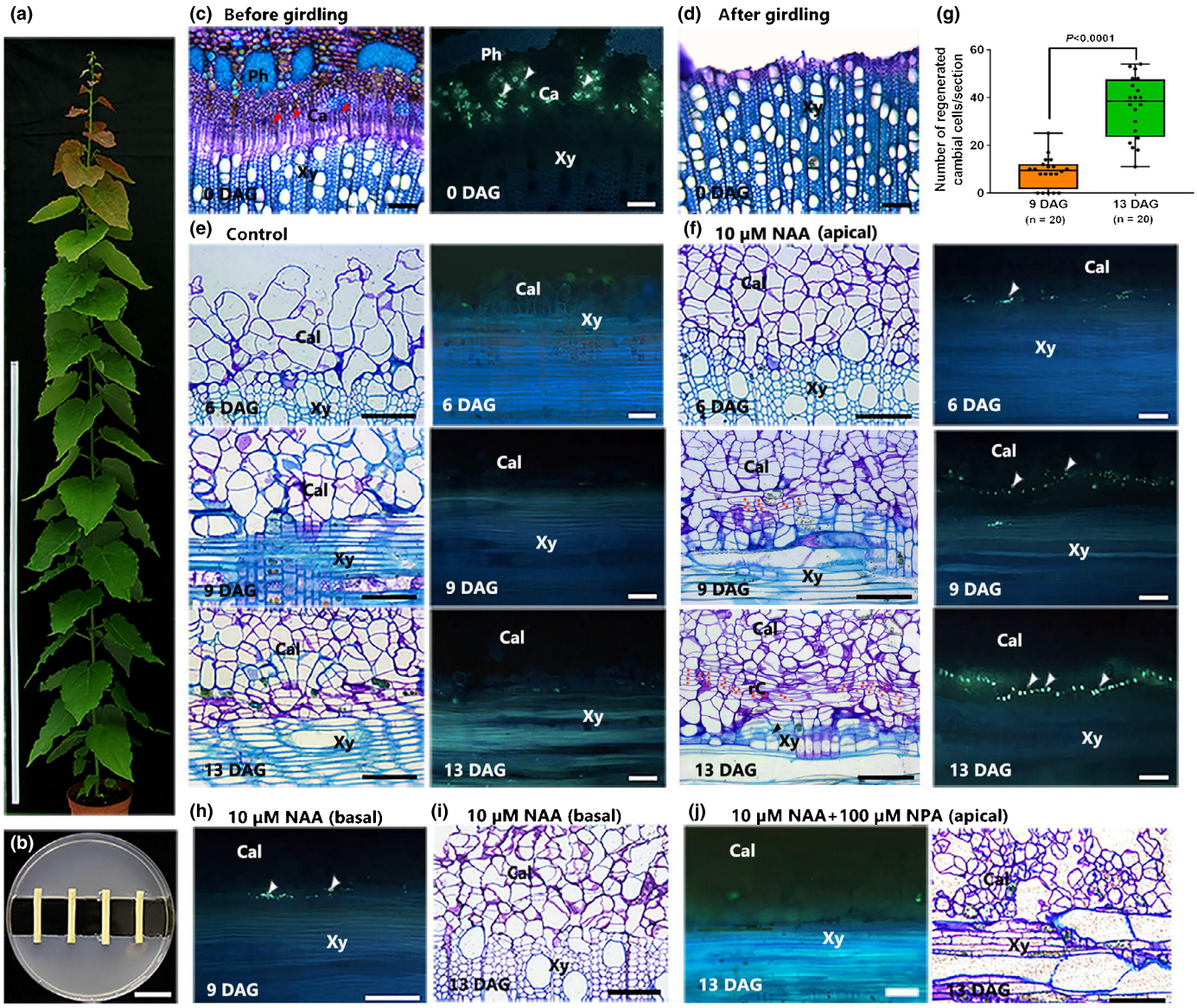

Fig. 1 Auxin stimulates the *in vitro* secondary vascular tissue (SVT) regeneration after bark girdling in *Populus* wild-type (WT) trees. (a) The *Populus tremula* × *Populus tremuloides* WT (clone T89) tree growing in the glasshouse used for the SVT regeneration experiment. (b) The sterile stem fragments incubated after girdling. (c) Toluidine blue O (TBO, left panel) and aniline blue (right panel) stained hand-cut cross-sections of the 30th stem internode in WT before girdling. (d) TBO-stained hand-cut cross-sections after girdling at 0 d after girdling (DAG). (e, f) TBO (left panel) stained plastic sections and aniline-blue-stained hand-cut longitudinal sections of the control stems (e) and 10 μM naphthaleneacetic acid (NAA)-incubated stems (f) at 6, 9 and 13 DAG. (g) Number of regenerated cambial cells per longitudinal section at 9 DAG and 13 DAG upon 10 μM NAA treatment as indicated in (f) with red asterisks. Box plots are centred at the median, which splits the first and third quartiles. *n*, number of sections used for quantification. *P* value was calculated using a two-tailed Student's *t*-test. (h) Aniline-blue-stained hand-cut longitudinal sections of stems treated with basally applied 10 μM NAA at 9 DAG. (i) TBO-stained plastic cross-sections of stems treated with apically applied 10 μM NAA at 13 DAG. (j) Aniline-blue-stained (left panel) hand-cut longitudinal sections and TBO-stained plastic longitudinal sections of stems treated with apically applied 10 μM NAA and 100 μM naphthylphthalamic acid (NPA) at 13 DAG. All TBO-stained sections were imaged with a bright-field microscope and all aniline-blue-stained sections were imaged with a fluorescence microscope. White arrowheads show the callose deposition stained by aniline blue. Red arrowheads show the original cambium in (c). Red asterisks show the regenerated cambial cells in (f). Black arrowheads show the regenerated xylem islands. Ph, phloem; Ca, cambium; Xy, xylem; Cal, callus; rC, regenerated cambium; 10 μM NAA (apical), 10 μM NAA applied in the apical part of the split-medium; 10 μM NAA (basal), 10 μM NAA applied in the basal part of the split-medium; 10 μM NAA + 100 μM NPA (apical), 10 μM NAA and 100 μM NPA applied in the apical part of the split-medium. Scale bars: 1 m in (a); 2 cm in (b); 100 μm in (c)–(f), (h)–(j).

both the cambium and phloem cells were peeled off, leaving only the differentiating xylem cells on the girdled stem surface (Fig. 1d). Thus, the original SVT pattern was disrupted after girdling.

At 3–6 DAG, callus cells derived from the differentiating xylem appeared and covered the girdled surface (Fig. 1e,f). With application of 10 μM NAA in the apical part of the split-medium, a patched callose accumulation was first detected at

6 DAG. A phloem sieve element (SE)-specific deposition pattern (i.e. callose deposition in sieve area and sieve plates along SEs; Pang *et al.*, 2008; Vatén *et al.*, 2011; Zhang *et al.*, 2011) was observed from 9 DAG (Fig. 1f). A new continuous cambium (i.e. at least four uninterrupted flat cambial cells adjacent to immature xylem cells that are undergoing periclinal division) was regenerated between 9 and 13 DAG (Fig. 1f,g). No regenerated cambial cells were observed at 6 DAG, and the number of regenerated cambial cells was significantly increased at 13 DAG (mean 36) compared with 9 DAG (mean 7.5; Fig. 1f,g). When a lower or higher concentration (5 or 25 μM) of NAA was applied, a similar pattern was observed except that no callose was detected upon 5 μM of NAA at 6 DAG (Fig. S1a–c). The average numbers of regenerated cambial cells at 13 DAG were 22.4 in 5 μM NAA-treated samples and 20.2 in 25 μM NAA-treated samples (Fig. S1c). Additionally, the observation of 'xylem islands' adjacent to the regenerated cambium at 13 DAG demonstrated that the newly formed cambium was active (Figs 1f, S1a,b). By contrast, when 10 μM NAA was applied in the basal part of the split-medium, the callose could be detected after 9 DAG (Fig. 1h) but no continuous cambial cells appeared at 13 DAG (Fig. 1i). When the auxin polar transport inhibitor *N*-1-naphthylphthalamic acid was applied together with NAA apically, no typical phloem SE or flat cambial cells were observed at 13 DAG (Fig. 1j). No obvious phloem or cambium was regenerated in the control samples (Figs 1e, S1d).

Based on these observations, we could conclude that the exogenous auxin is sufficient to induce SVT regeneration *in vitro* and that phloem is regenerated before the formation of a functional cambium in this system. These results also imply that auxin transport may influence the regeneration of cambium, since SVT regeneration only occurred when auxin was added to the apical part of the medium (Fig. 1f,g).

Expression analysis of the vascular marker genes verified the tissue identities during the *in vitro* SVT regeneration

To further define the various stages of the SVT regeneration process, we identified and investigated various vascular tissue identity marker genes in *Populus*. It is well known that *APL* is a major transcription factor that regulates phloem identity and is specifically expressed in phloem (Bonke *et al.*, 2003). In addition, *CALS7* is phloem specific and responsible for callose deposition in the SEs (Xie *et al.*, 2011). Orthologues of *AtAPL* and *AtCALS7* were identified in the *Populus* genome, named *PtAPL-1*, *PtAPL-2*, *PtCALS7-1* and *PtCALS7-2* (Figs S2, S3). Expression of these four genes was examined across the *Populus* cambial zone in sequential cryosections (Nieminen *et al.*, 2008) by qRT-PCR. The results demonstrated that their expression levels peaked in early phloem (Fig. S4). *PtAPL-1* and *PtCALS7-1* were selected as phloem markers in *Populus* and their expression patterns investigated during SVT regeneration. Upon 10 μM NAA treatment, the expression levels of both *PtAPL-1* and *PtCALS7-1* were significantly increased after 6 DAG and continuously upregulated until 13 DAG, when there was a steep increase (Fig. 2a,b), probably because the newly formed cambium started to produce new phloem (Figs 1, 2a,b). By contrast, the expression of neither gene was induced in the control samples (Fig. 2a,b). Our data confirmed that auxin induced the restoration of phloem identity as early as 6 DAG.

We next verified the new cambium identity during the SVT regeneration process by using the *Populus* transgenic line harbouring the GUS reporter of *AINTEGUMENTA-LIKE-1* (*PtAIL1*), referred to as *pAIL1:GUS* (Karlberg *et al.*, 2011). *PtAIL1* has been identified as the *Populus* orthologue of the *Arabidopsis* transcription factor *AINTEGUMENTA* (*ANT*) that is specifically expressed in cambium (Randall *et al.*, 2015). We first checked the expression patterns of *PtAIL1* before girdling and found that it was enriched in the cambium zone and the primary xylem parenchyma cells in the stem (Fig. 2c). After girdling, the GUS signals disappeared, indicating the removal of original cambium (Fig. 2c). During SVT regeneration, in the 10 μM NAA-incubated samples, a GUS signal was detected at 3 and 6 DAG at a very low level, and then became more visible at 9 DAG (Fig. 2e). At 13 DAG, a strong GUS signal was observed in the regenerated cambium region, resembling the pattern before girdling (Fig. 2e). The GUS signal in the control treatment remained at a very low level throughout the whole process (Fig. 2d).

Collectively, by analysing the expression patterns of the vascular marker genes across the *in vitro* SVT regeneration process induced by auxin, we confirmed the molecular identities of the regenerated tissues at various regeneration stages, which were consistent with our morphological observations (Fig. 1).

CK is sufficient to induce new phloem but not cambium regeneration

To investigate the potential roles of CK in SVT regeneration, we applied tZ to WT *Populus* samples during *in vitro* incubation. With 1 μM tZ treatment, callose could be detected in the cells adjacent to xylem cells as early as 3 DAG, and the phloem-specific deposition pattern appeared at 13 DAG (Fig. 3b). Starting from 9 DAG, there was also detectable callose deposition in the sample incubated with 0.1 μM tZ (Fig. S5a). However, only weak signals could be found with 10 μM or 60 μM tZ application at 13 DAG (Fig. S5b,c). These results indicated that CK could stimulate the phloem regeneration in a dose-dependent manner during SVT regeneration.

Analysis of the expression patterns of *PtAPL-1* showed that it was highly induced at 3 DAG (Fig. 4a), earlier than in NAA-treated samples (Fig. 2a). For *PtCALS7-1*, the expression was induced from 3 DAG until 13 DAG (Fig. 4a). These data were in agreement with the callose deposition phenotypes (Fig. 3b) and validated that CK could promote phloem regeneration.

Moreover, to verify the role of CK during SVT regeneration genetically, we generated and used multiple transgenic trees in which CK signalling or biosynthesis was manipulated. To stimulate the CK signalling in vascular tissues, we overexpressed the *AtCKI1* gene under the *PttLMX5* promoter (Love *et al.*, 2009). It has been reported that *AtCKI1* induces the CK-independent activation of CK signalling during vascular bundle development in

New Phytologist

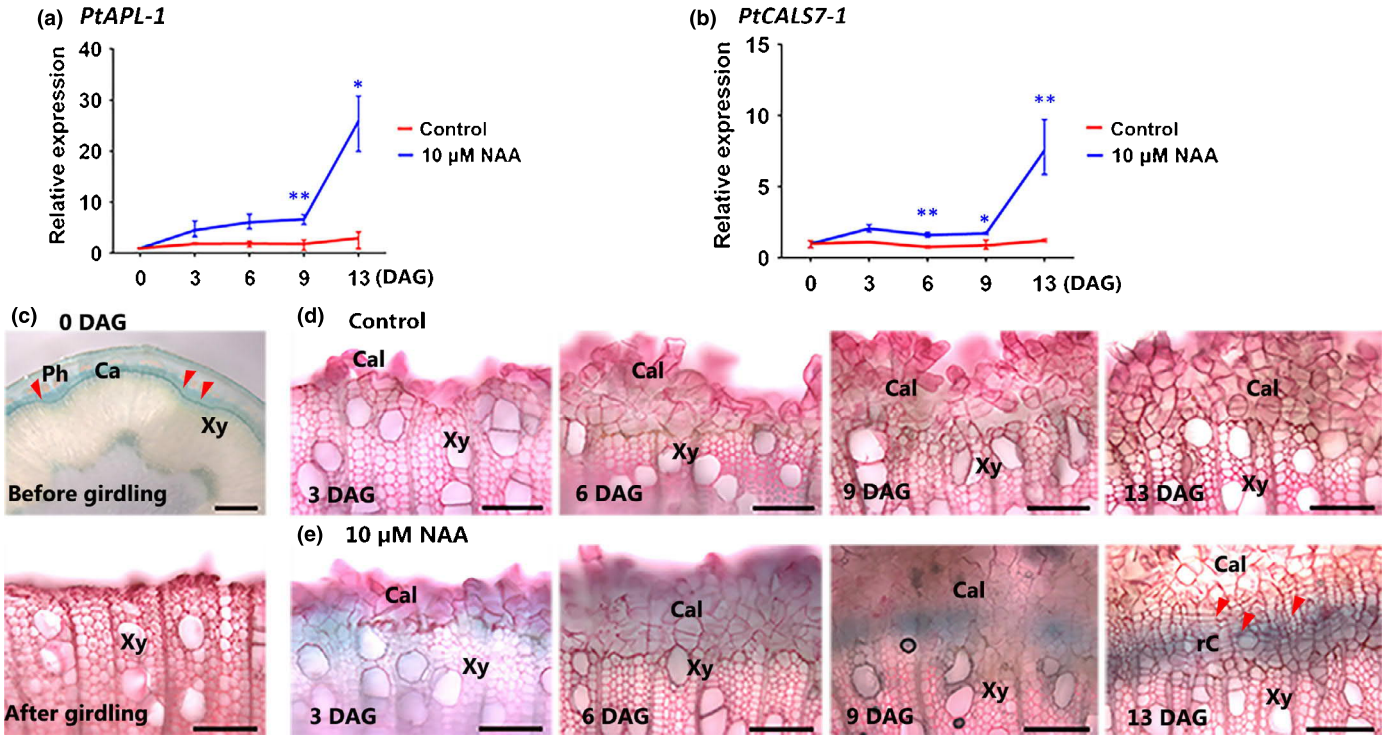

Fig. 2 The expression of the secondary vascular tissue markers during regeneration upon auxin treatment in *Populus* validates the identities of regenerated tissues. The transcriptional expression of (a) *PtAPL-1* and (b) *PtCALS7-1* at 0, 3, 6, 9 and 13 d after girdling (DAG) in the control or 10 μM naphthaleneacetic acid (NAA) incubated wild-type samples. Gene expression was quantified by quantitative reverse transcription PCR. Relative expression is normalized against the expression of 0 DAG. Value is mean ± SE ($n = 3$). Student's *t*-test was done between the NAA-treated sample and control sample at each stage. **, $P < 0.01$; *, $P < 0.05$. The exact *P* value for each comparison can be found in Supporting Information Table S2. (c) The β-glucuronidase (GUS) expression in *pAIL1:GUS* transgenic lines before girdling (upper panel) and after girdling (lower panel) at 0 DAG. GUS-stained hand-cut sections from the 30th stem internode are shown. (d) GUS expression in the hand-cut sections of control *pAIL1:GUS* transgenic lines at 3, 6, 9 and 13 DAG. (e) GUS expression in the 10 μM NAA-incubated *pAIL1:GUS* transgenic lines at 3, 6, 9 and 13 DAG. All sections were imaged with a bright-field microscope in (c)–(e). The red arrowheads show the newly formed continuous flat cambium cells. Ph, phloem; Ca, cambium; Xy, xylem; Cal, callus; rC, regenerated cambium. Scale bars, 100 μm.

Arabidopsis (Hejatko *et al.*, 2009). Among the 10 transgenic lines we investigated, *PttLMX5::AtCKI1* lines 1 and 7 both showed high induction levels of *AtCKI1* and type-A CK response regulator *PtRR7* compared with WT (Fig. S6), indicating that CK signalling was elevated in these two transgenic lines. Line 1 was selected for further SVT regeneration study. Another two transgenic lines reported previously, *PttLMX5::AtIPT7* (Immanen *et al.*, 2016) and *pBpCRE1::AtCKX2* (Nieminen *et al.*, 2008), in which CK biosynthesis is respectively increased and decreased, were also investigated during SVT regeneration. We observed that phloem-like callose deposition appeared at 13 DAG without any exogenous CK treatment in both *PttLMX5::AtCKI1* and *PttLMX5::AtIPT7* lines (Fig. 5a,b). By contrast, callose deposition was induced in *pBpCRE1::AtCKX2* line at 6 DAG only upon treatment with a higher concentration of CK (10 μM tZ; Fig. 5c) than in the WT (Fig. 3). These observations confirmed that elevated CK signalling or hormone content promotes phloem regeneration, whereas the lack of CK causes defects in this process.

Surprisingly, anatomic analysis revealed that no cambium was observed with CK application even at a late stage (13 DAG; Figs 3b, S5). This absence of cambium was also found in the *PttLMX5::AtCKI1*, *PttLMX5::AtIPT7* and *pBpCRE1::AtCKX2* trees. These anatomic results were in line with the observation of a cambium marker reporter line (Fig. 4c). In the *pAIL1:GUS* line, similar to the control samples (Fig. 4b), only weak GUS signals were found in the xylem cells near the girdled surface in the CK-treated samples at 3 DAG and no distinct signals were observed in later stages (Fig. 4c). These data together indicated that CK alone might not be sufficient to induce cambium regeneration in this *in vitro* system.

The interaction between auxin and CK affects SVT regeneration

As already described, our study showed that exogenous application of auxin alone was sufficient to induce both phloem and cambium regeneration (Figs 1, S1), whereas CK contributed to the phloem repatterning but not the cambium reconstruction (Figs 3, 5, S5). Based on the distinct effects of exogenously added auxin and CK during SVT regeneration, we next investigated the interaction between these two hormones during this process. To this end, WT stems were girdled and incubated in medium containing combinatorial 10 μM NAA and 1 μM tZ. Phloem-specific callose deposition was detected from 6 DAG, and the signals were enhanced along regeneration (Fig. 3c). The expression of

COLOR

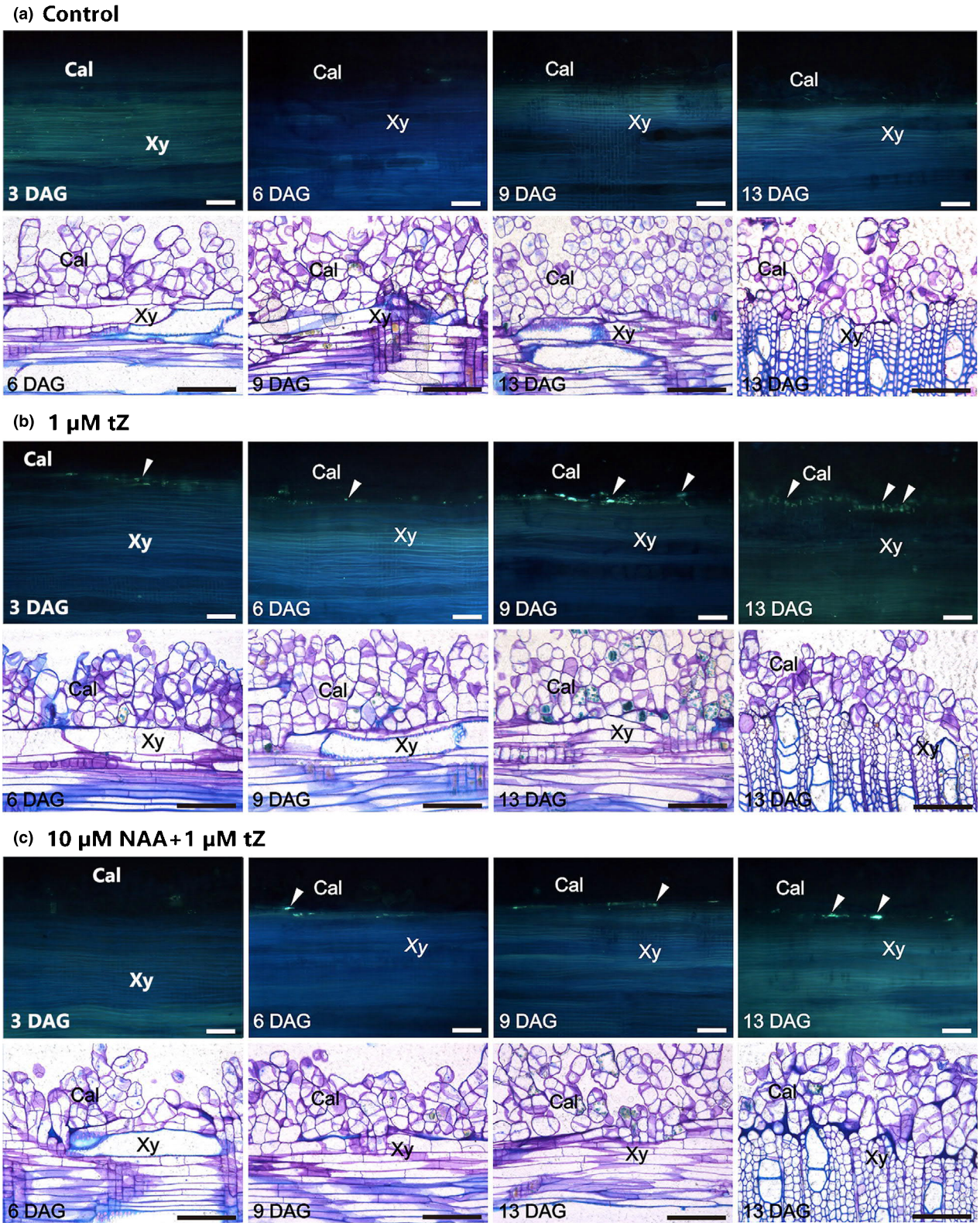

Fig. 3 Phloem repatterning induced by cytokinin during *in vitro* secondary vascular tissue regeneration after bark girdling in *Populus* wild-type (WT) trees. (a)–(c) Aniline-blue-stained hand-cut longitudinal sections (upper panel) and toluidine blue O (TBO)-stained plastic longitudinal- (3–13 d after girdling, DAG) or cross-sections (13 DAG) (lower panel) of (a) the control or (b) 1 μM *trans*-zeatin (tZ) or (c) 1 μM tZ and 10 μM naphthaleneacetic acid (NAA)-incubated WT stems at 3, 6, 9 and 13 DAG. TBO-stained sections were imaged with a bright-field microscope, and aniline-blue-stained sections were imaged with a fluorescence microscope. The white arrowheads show the callose deposition stained by aniline blue. Cal, callus; Xy, xylem. Scale bars, 100 μm.

New Phytologist

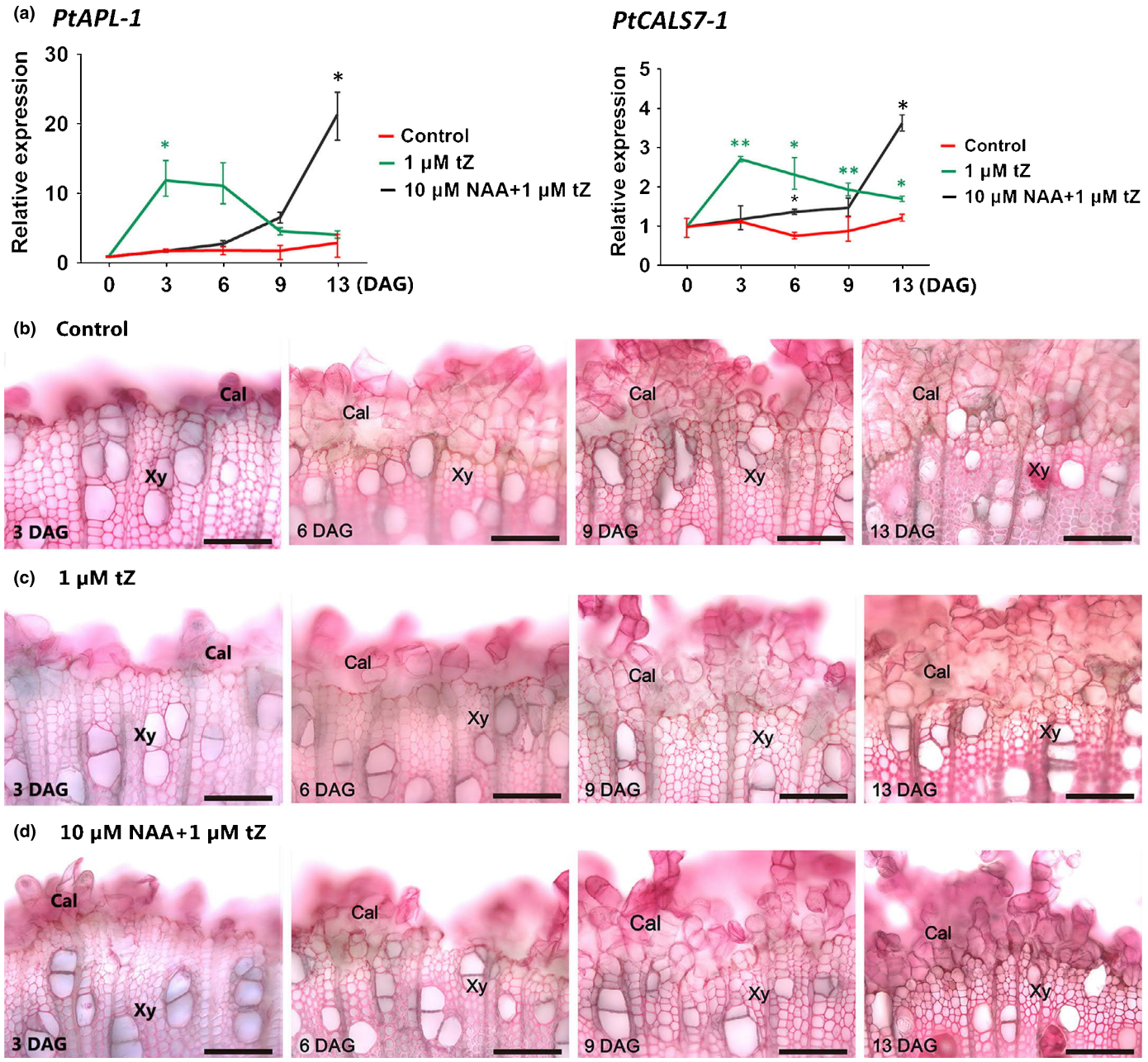

Fig. 4 The expression of the secondary vascular tissue (SVT) markers during the *in vitro* SVT regeneration upon cytokinin or combinatorial auxin and cytokinin treatment in *Populus*. (a) The transcriptional expression of *PtAPL-1* and *PtCALS7-1* at 0, 3, 6, 9 and 13 d after girdling (DAG) in the control or 1 μM *trans*-zeatin (tZ) or 10 μM naphthaleneacetic acid (NAA) and 1 μM tZ-incubated samples. Gene expression was quantified by quantitative reverse transcription PCR. Relative expression is normalized against the expression of 0 DAG. Value is mean ± SE ($n = 3$). Student's *t*-test was done between the NAA-treated sample and control sample at each stage. **, $P < 0.01$; *, $P < 0.05$. The exact *P* value for each comparison can be found in Supporting Information Table S2. (b)–(d) β-Glucuronidase (GUS expression in the stems of pAIL1:GUS at 3, 6, 9 and 13 DAG upon (b) the control treatment, (c) 1 μM tZ treatment and (d) 1 μM tZ and 10 μM NAA treatment. All GUS-stained hand-cut sections were imaged with a bright-field microscope. Cal, callus; Xy, xylem. Scale bars, 100 μm.

PtCALS7-1 was significantly upregulated from 6 DAG, whereas the increase of *PtAPL* expression became significant only at 13 DAG (Fig. 4a).

Interestingly, with combinatorial auxin and CK treatment, there was no continuous cambium formation (Fig. 3c) and no distinct GUS signal detected in *pAIL1:GUS* line at all stages (Fig. 4d), which resembled the phenotypes in the sample treated with CK alone (Fig. 4c). These results indicated that CK might inhibit cambium regeneration even in the presence of exogenous auxin in the *in vitro* SVT regeneration system.

To further study the interaction between auxin and CK during SVT regeneration, the expression profiles of auxin response factor *PtIAA3* and CK response regulator *PtRR7*

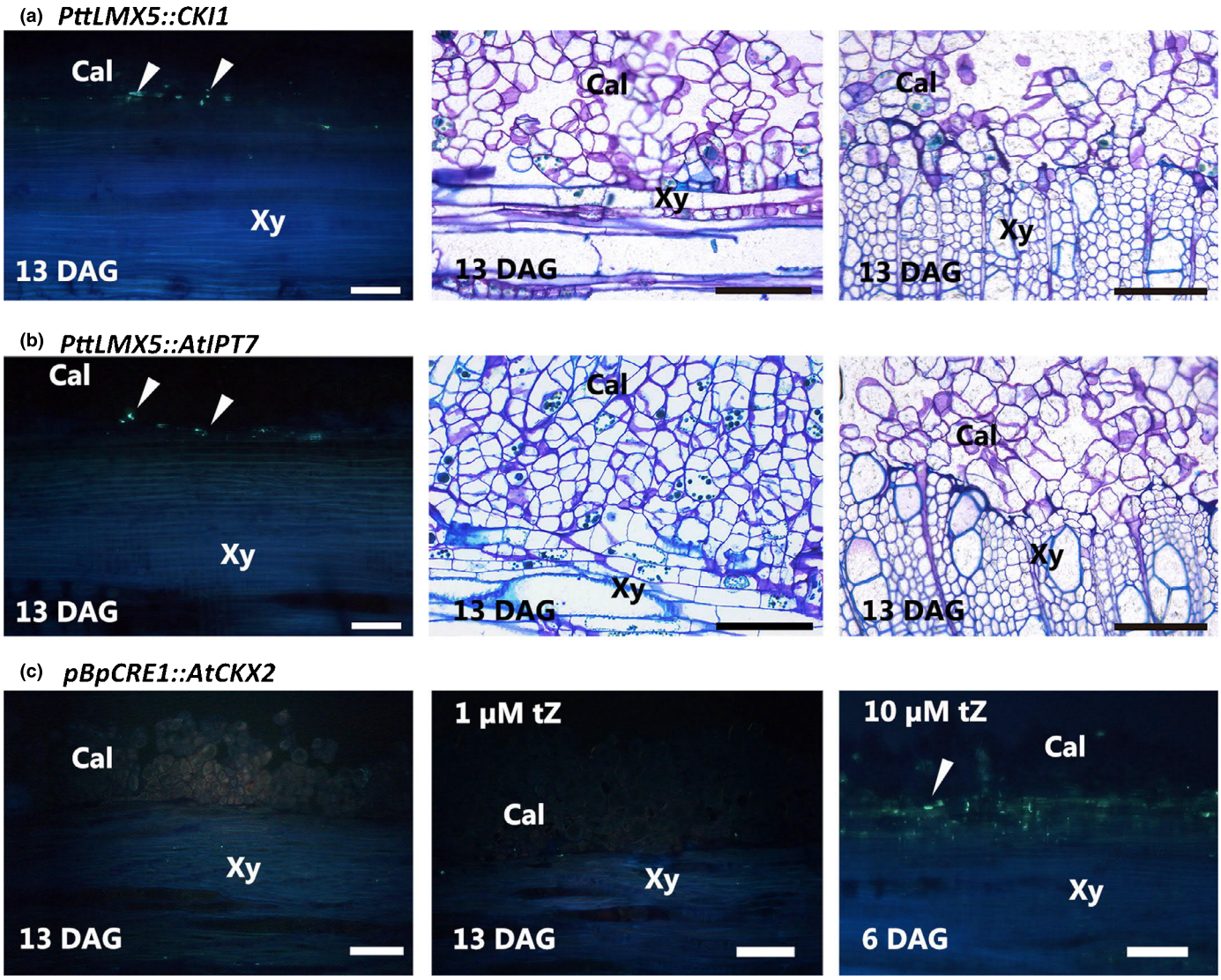

Fig. 5 Phloem re-establishment during the *in vitro* secondary vascular tissue regeneration after bark girdling in cytokinin-altered transgenic tree lines. Aniline-blue-stained hand-cut longitudinal section (left) and toluidine blue O (TBO)-stained plastic longitudinal- (middle) and cross-sections (right) of (a) the *PttLMX5::CKI1* transgenic line and (b) *PttLMX5::AtIPT7* transgenic line stems at 13 d after girdling (DAG). (c) Aniline-blue-stained hand-cut longitudinal sections of the *pBpCRE1::AtCKX2* stems upon the control treatment (left), 1 μM *trans*-zeatin (tZ) treatment (middle) and 10 μM tZ treatment (right) at 13 DAG. TBO-stained sections were taken with a bright-field microscope, and aniline-blue-stained sections were taken with a fluorescence microscope. The white arrowheads show the fluorescence signals stained by aniline blue. Cal, callus; Xy, xylem. Scale bars, 100 μm.

were analysed. *PtIAA3* was induced dramatically with 10 μM NAA treatment from 3 DAG and reached a maximum at 6 DAG, whereas it was inhibited with 1 μM tZ and control treatment from 3 DAG (Fig. 6f). In the case of joint treatment of NAA and tZ, *PtIAA3* was slightly induced at 3 DAG but then dropped during regeneration (Fig. 6f). For *PtRR7*, it was induced by tZ treatment and reached a maximum at 3 DAG. Interestingly, *PtRR7* was also significantly increased upon NAA treatment at 3 DAG before phloem regeneration. However, the increase of *PtRR7* was not detected when treated with both NAA and tZ (Fig. 6g).

Taken together, these results indicated that auxin could activate CK signalling in the early stage of regeneration whereas the elevated CK might negatively regulate auxin signalling.

Auxin gradient redistribution is required for cambium re-establishment during SVT regeneration

It is well known that a radial auxin concentration gradient across SVTs in trees is important for vascular patterning (Uggla *et al.*, 1996; Immanen *et al.*, 2016), and this gradient is believed to be achieved through polar auxin transport (Schrader *et al.*, 2003). Therefore, it is speculated that the reconstruction of an auxin gradient is crucial for SVT regeneration. To test this hypothesis, we used a *Populus* auxin-responsive DR5 reporter line, *PtaDR5:GUS*, to visualize the auxin response during the re-establishment of phloem and cambium.

Before girdling, the GUS expression was mainly observed in the cambium zone (Fig. 6a), confirming the previous findings

New Phytologist

COLOR

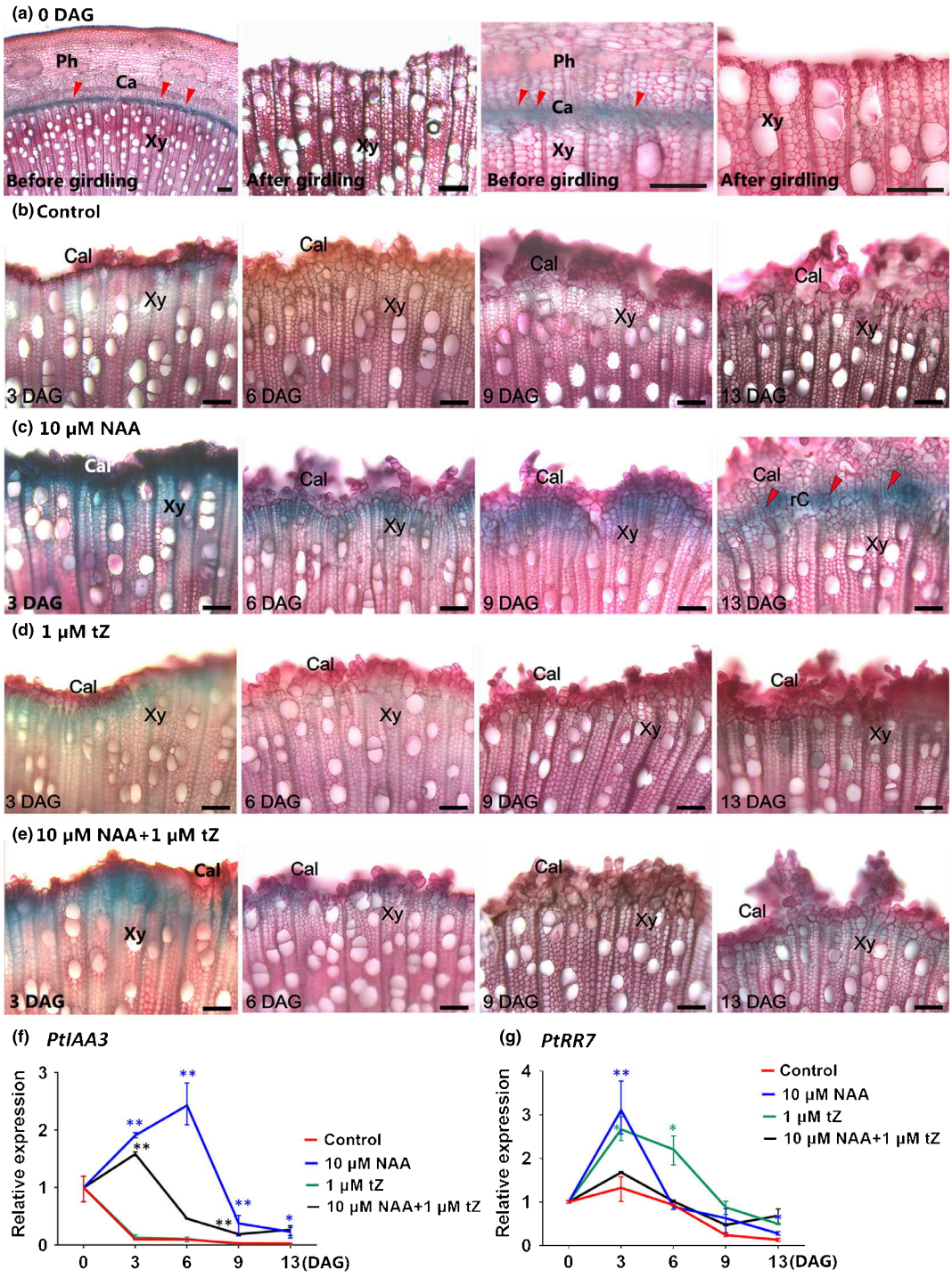

Fig. 6 The auxin gradient redistribution in *PtaDR5:GUS* line and the expression pattern of *PtIAA3* and *PtRR7* during the *in vitro* secondary vascular tissue (SVT) regeneration. (a) The β-glucuronidase (GUS) expression in *PtaDR5:GUS* transgenic lines before and after girdling at 0 d after girdling (DAG). GUS-stained hand-cut sections staining from the 30th stem internode are shown. GUS expression in the hand-cut sections of *PtaDR5:GUS* stems at 3, 6, 9 and 13 DAG upon (b) the control treatment, (c) 10 μM naphthaleneacetic acid (NAA) treatment, (d) 1 μM *trans*-zeatin (tZ) treatment and (e) 10 μM NAA and 1 μM tZ treatment. All sections were imaged with a bright-field microscope. The red arrowheads show the restored continuous flat cambium cells. Ph, phloem; Ca, cambium; Xy, xylem; Cal, callus; rC, regenerated cambium. Scale bars, 100 μm. The transcriptional expression of (f) *PtIAA3* and (g) *PtRR7* at 0, 3, 6, 9 and 13 DAG during SVT regeneration stimulated by various hormonal treatments. Note that the lines for control and tZ treatments overlap in (f). Gene expression was quantified by quantitative reverse transcription PCR. Relative expression is normalized against the expression of 0 DAG. Value is mean ± SE ($n = 3$). Student's *t*-test was done between the NAA-treated sample and control sample at each stage. **, $P < 0.01$; *, $P < 0.05$. The exact *P* value for each comparison can be found in Supporting Information Table S2.

(Spicer *et al.*, 2013). The GUS signals disappeared right after bark girdling (Fig. 6a), indicating a disruption of the auxin gradient across the SVT. GUS expression was induced in the xylem region below the surface at 3 DAG in all samples, including the control sample (Fig. 6b–e), suggesting a wounding-induced auxin response. However, it is notable that the signals were strongest in the sample treated with 10 μM NAA at 3 DAG. During later stages of regeneration, the DR5 signal was first decreased at 6–9 DAG and was then confined to the region where the regenerated cambium appeared at 13 DAG upon auxin treatment (Fig. 6c), mimicking the patterns in the WT before girdling (Fig. 6a). Conversely, the GUS expression was below detection in the control samples after 3 DAG (Fig. 6b). Similarly, the signal was greatly reduced in CK and in auxin and CK jointly treated samples (Fig. 6d,e) at later stages (6–13 DAG), suggesting that the new auxin maximum domain was not built up under these conditions. Therefore, lack of DR5 expression was coincident with the failure of cambium restoration, implying the essential role of auxin redistribution during SVT regeneration. The data also suggested that CK may block the re-establishment of an auxin maximum, which is required for the new cambium formation.

Discussion

The roles of phytohormones have been widely studied in various plant regeneration systems as well as in SVT development. However, it has been difficult to investigate how hormones regulate SVT regeneration in trees due to the limitation of using field-grown trees (Chen *et al.*, 2014). We herein report a new *in vitro* SVT regeneration system in *Populus* to explore the roles of auxin and CK in regulation of SVT regeneration.

In agreement with the findings in several other plant regeneration or organogenesis systems (reviewed by Chen *et al.*, 2014), we found that auxin is crucial for the SVT regeneration process. Without exogenous auxin application in the *in vitro* system, only callus formation was observed and no SVT regeneration occurred (Figs 1e, 2d, 3a, 4b, 6b). With auxin treatment, both phloem and cambium were restored sequentially and derived from differentiating xylem after girdling, similar to what is observed in the *in situ* SVT regeneration system (Zhang *et al.*, 2011). It is well known that there is an auxin gradient across the wood formation zone with the peak in the cambium (Uggla *et al.*, 1998; Immanen *et al.*, 2016). This is also confirmed by checking the DR5 signals along the SVT zones (Spicer *et al.*, 2013; Fig. 6a). By employing the *PtaDR5:GUS* line, we were able to visualize the auxin response during SVT regeneration. Our data revealed that the radial auxin distribution destroyed by girdling is restored preceding the respecification of cambium upon auxin treatment but not on CK or combinatorial auxin and CK treatments. These data suggested auxin is sufficient to induce the regeneration of both phloem and cambium from the residual xylem cells after girdling and that the redistribution of an auxin gradient across the cambium zone is required for cambium reformation.

To our surprise, we discovered that exogenous CK alone could induce phloem regeneration (Fig. 3). This finding was confirmed by using transgenic trees in which CK signalling (*PttLMX5::AtCKI1*) or content (*PttLMX5::AtIPT7*) was elevated (Fig. 5a,b). On the other hand, when CK concentration was reduced in *pBpCRE1::AtCKX2* trees, the fact that more exogenous CK was needed to stimulate the phloem reformation (Fig. 5c) suggested CK is required for phloem regeneration. A recent report showed that CKs peak in the developing phloem tissue and that the CK response domains are consistent with the hormonal gradients revealed by genome-wide gene expression profiling (Immanen *et al.*, 2016). Both our data and the published data demonstrated that CK is important for phloem development and phloem regeneration. Intriguingly, in the samples with CK treatment or auxin and CK joint treatment, cambium regeneration did not occur. The absence of cambium was also found in the *PttLMX5::CKI1* or *PttLMX5::AtIPT7* trees during SVT regeneration. On the other hand, it is already known that CK is required for vascular cambium development, since radial growth is dramatically reduced in *pBpCRE1::AtCKX2* trees (Nieminen *et al.*, 2008). Therefore, CK appears to promote cambium activity in the presence of a cambium in intact trees but inhibit the establishment of new cambium during SVT regeneration.

Taken together, we herein propose a hormonal regulatory model during SVT regeneration based on current observations (Fig. 7). We have demonstrated previously, in early regeneration (3 DAG), residual xylem axial cells (vessel and fibre) gained the

COLOR

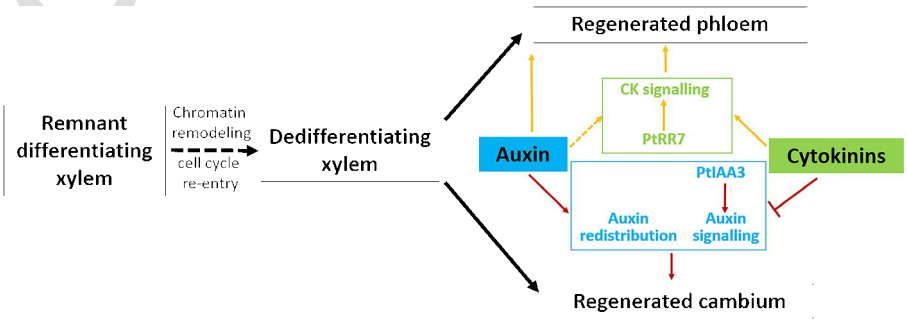

Fig. 7 Proposed hormonal regulatory model of the *in vitro* secondary vascular tissue (SVT) regeneration. Based on our observations, we propose that, after girdling, both phloem and cambium are regenerated from the remnant differentiating xylem cells during SVT regeneration in *Populus* stems. Both auxin and cytokinin (CK) regulate the restoration of phloem and cambium. Auxin alone can induce both phloem and cambium formation, whereas CK promotes only phloem formation and inhibits cambium regeneration, probably by inhibiting auxin redistribution and signalling. On the other hand, auxin may stimulate phloem repatterning by inducing *PtRR7* through the CK signalling pathway.

ability to divide periclinally and dedifferentiate into a meristematic stage preceding the re-establishment of phloem and cambium (Pang *et al.*, 2008; Zhang *et al.*, 2011). It has been reported very recently that xylem acts as the cambium stem-cell organizer in the *Arabidopsis* root (Smetana *et al.*, 2019). Our findings that phloem and cambium are re-specified from the remaining differentiating xylem after girdling thus validate the role of xylem as organizer during SVT regeneration. Furthermore, our investigation supported the hypothesis that complementary auxin and CK domains are required for phloem and cambium reconstruction. For phloem recovery, high CK and lower auxin domains are necessary; for cambium regeneration, however, high auxin and lower CK domains are essential (see the following).

Although both auxin and CK alone induced phloem formation, the expression of *PtRR7* indicated that auxin might induce phloem formation while activating CK signalling (Fig. 6g). It is reported that *PtRR7* is abundantly expressed in phloem cells (Immanen *et al.*, 2016), so the observation that dual treatment of NAA and tZ cannot induce *PtRR7* (Fig. 6g) might be due to the fact that fewer phloem cells expressing *PtRR7* were formed in this condition. When CK signalling or biosynthesis was elevated via overexpressing either *AtCKI1* or *AtIPT7*, phloem was regenerated without any hormone treatment. By contrast, when the CK level was reduced in *AtCKX2*-overexpression trees, a higher concentration of CK was required for phloem recovery. These results support the suggestion that phloem is regenerated within a high endogenous CK domain. On the other hand, lower auxin level was observed in the *PtaDR5:GUS* line before the appearance of phloem *c.* 6 DAG. It was also speculated earlier that phloem regeneration may require less auxin because the auxin level is lower in the position where phloem would appear in the early stage of regeneration in *Eucommia* trees (Mwange *et al.*, 2003). Furthermore, both the DR5 signals and the expression of *PtIAA3* were significantly decreased upon CK treatment compared with auxin treatment before phloem regeneration at 6 DAG. These data suggest that CK might inhibit the auxin signalling to maintain a lower auxin domain during phloem reconstruction (Fig. 7).

For cambium reformation, a high endogenous auxin domain seemed essential, as seen in the normal growing trees (Uggla *et al.*, 1998; Immanen *et al.*, 2016; Fig. 6c). DR5 signal was increased before cambium recovery and then restricted to the newly established cambium domain upon auxin treatment. Conversely, DR5 signal disappeared upon CK application after 6 DAG, and, as a consequence, no cambium was regenerated, indicating that an auxin maximum was required for cambium restoration. Interestingly, *PtIAA3* was largely inhibited upon CK treatment from 3 DAG, implying that auxin signalling was low in CK-treated samples and therefore no cambium could form. All of the aforementioned evidence indicated that no cambium could reoccur without a high auxin domain. The fact that *PtRR7* was decreased before cambium regeneration on auxin treatment indicated a lower CK domain at the cambium zone. Based on these data, we propose that both high auxin and low CK domains are required for cambium regeneration (Fig. 7). When the CK level was high in either hormone-treated samples or *AtCKI1* and *AtIPT7* overexpressing trees, no cambium was reformed. In the case of dual treatment of auxin and CK, no cambium occurred either.

In conclusion, such complementary endogenous domains of auxin and CK might provide positional information for the secondary vascular tissue regeneration. Perturbation of such information may lead to failure of tissue regeneration. Future efforts will focus on using this *in vitro* system to trace the sequential cellular events and dissect the interactions between the key regulatory factors at a cellular level during SVT regeneration process. As shown decades ago, mechanical pressure could be a crucial factor for SVT differentiation and regeneration (Brown & Sax, 1962), and our *in vitro* system could thus be modified to explore the roles of other factors, in addition to the molecular regulators, during tissue regeneration.

Acknowledgements

We thank Rishikesh P. Bhalerao (Umeå Plant Science Center) for providing *pAIL1:UidA* (*pAIL1:GUS*) transgenic trees and Katja Kainulainen (University of Helsinki) for the excellent technical assistance. This work was supported by the National key research and development program of China (2016YFD0600103), the National Natural Science Foundation of China (31570581) and the Finnish Centre of Excellence in Molecular Biology of Primary Producers (Academy of Finland CoE program). No conflict of interest declared.

Author contributions

J-JC, L-YW, JI, KN and RS performed experiments and assisted with data analyses. X-QH, JZ, YH, J-JC and L-YW designed the experiments and analysed and interpreted the data. JZ, J-JC and X-QH wrote the manuscript. All authors read and commented on the manuscript. J-JC and L-YW contributed equally to this work.

ORCID

Xin-Qiang He https://orcid.org/0000-0002-1755-008X
Ykä Helariutta https://orcid.org/0000-0002-7287-8459
Juha Immanen https://orcid.org/0000-0003-1098-4843
Kaisa Nieminen https://orcid.org/0000-0001-7004-9422
Rachel Spicer https://orcid.org/0000-0002-1129-3932
Jing Zhang https://orcid.org/0000-0003-4463-7516

References

Agusti J, Lichtenberger R, Schwarz M, Nehlin L, Greb T. 2011. Characterization of transcriptome remodeling during cambium formation identifies *MOL1* and *RUL1* as opposing regulators of secondary growth. *PLoS Genetics* 7: e1001312.

Bhalerao RP, Fischer U. 2014. Auxin gradients across wood-instructive or incidental? *Physiologia Plantarum* **151**: 43–51.

Bonke M, Thitamadee S, Mahonen AP, Hauser MT, Helariutta Y. 2003. APL regulates vascular tissue identity in *Arabidopsis*. *Nature* **426**: 181–186.

Brown CL, Sax K. 1962. The influence of pressure on the differentiation of secondary tissues. *American Journal of Botany* **49**: 683–691.

Che P, Lall S, Howell SH. 2007. Developmental steps in acquiring competence for shoot development in *Arabidopsis* tissue culture. *Planta* **226**: 1183–1194.

Chen LQ, Sun BB, Xu L, Liu W. 2016a. Wound signaling: the missing link in plant regeneration. *Plant Signaling & Behavior* **11**: e1238548.

Chen LQ, Tong JH, Xiao LT, Ruan Y, Liu JC, Zeng MH, Huang H, Wang JW, Xu L. 2016b. *YUCCA*-mediated auxin biogenesis is required for cell fate transition occurring during *de novo* root organogenesis in *Arabidopsis*. *Journal of Experimental Botany* **67**: 4273–4284.

Chen JJ, Zhang J, He XQ. 2014. Tissue regeneration after bark girdling: an ideal research tool to investigate plant vascular development and regeneration. *Physiologia Plantarum* **151**: 147–155.

Cheng ZJ, Wang L, Sun W, Zhang Y, Zhou C, Su YH, Li W, Sun TT, Zhao XY, Li XG *et al.* 2013. Pattern of auxin and cytokinin responses for shoot meristem induction results from the regulation of cytokinin biosynthesis by AUXIN RESPONSE FACTOR3. *Plant Physiology* **161**: 240–251.

Correa LD, Troleis J, Mastroberti AA, Mariath JEA, Fett AG. 2012. Distinct modes of adventitious rooting in *Arabidopsis thaliana*. *Plant Biology* **14**: 100–109.

Cui KM, Lu PZ, Liu QH, Li ZG. 1989. Regeneration of vascular tissues in *Broussonetia papyrifera* stems after removal of the xylem. *IAWA Bulletin* **10**: 193–199.

Cui KM, Wu SQ, Wei LB, Little CHA. 1995. Effect of exogenous IAA on the regeneration of vascular tissues and periderm in girdled *Betula pubescens* stems. *Chinese Journal of Botany* **7**: 17–23.

Du J, Xie HL, Zhang DQ, He XQ, Wang MJ, Li YZ, Cui KM, Lu MZ. 2006. Regeneration of the secondary vascular system in poplar as a novel system to investigate gene expression by a proteomic approach. *Proteomics* **6**: 881–895.

Efroni I, Mello A, Nawy T, Ip PL, Rahni R, DelRose N, Powers A, Satija R, Birnbaum KD. 2016. Root regeneration triggers an embryo-like sequence guided by hormonal interactions. *Cell* **165**: 1721–1733.

Gordon SP, Chickarmane VS, Ohno C, Meyerowitz EM. 2009. Multiple feedback loops through cytokinin signaling control stem cell number within the *Arabidopsis* shoot meristem. *Proceedings of the National Academy of Sciences, USA* **106**: 16529–16534.

Haberlandt G. 1902. Culturversuche mit isolierten Pflanzenzellen. *Sitzungsberichte der Mathematisch-Naturwissenschaftlichen Classe der Kaiserlichen Akademie der Wissenschaften. Abteilung 1, Mineralogie, Botanik, Zoologie, Anatomie, Geologie, Paläontologie* **111**: 69–92.

Hejatko J, Ryu H, Kim GT, Dobesova R, Choi S, Choi SM, Soucek P, Horak J, Pekarova B, Palme K *et al.* 2009. The histidine kinases CYTOKININ-INDEPENDENT1 and ARABIDOPSIS HISTIDINE KINASE2 and 3 regulate vascular tissue development in *Arabidopsis* shoots. *Plant Cell* **21**: 2008–2021.

Ikeuchi M, Ogawa Y, Iwase A, Sugimoto K. 2016. Plant regeneration: cellular origins and molecular mechanisms. *Development* **143**: 1442–1451.

Immanen J, Nieminen K, Smolander OP, Kojima M, Serra JA, Koskinen P, Zhang J, Elo A, Mahonen AP, Street N *et al.* 2016. Cytokinin and auxin display distinct but interconnected distribution and signaling profiles to stimulate cambial activity. *Current Biology* **26**: 1990–1997.

Iwase A, Harashima H, Ikeuchi M, Rymen B, Ohnuma M, Komaki S, Morohashi K, Kurata T, Nakata M, Ohme-Takagi M *et al.* 2017. WIND1 promotes shoot regeneration through transcriptional activation of *ENHANCER OF SHOOT REGENERATION1* in Arabidopsis. *Plant Cell* **29**: 54–69.

Kakani A, Li GS, Peng Z. 2009. Role of AUX1 in the control of organ identity during *in vitro* organogenesis and in mediating tissue specific auxin and cytokinin interaction in *Arabidopsis*. *Planta* **229**: 645–657.

Karlberg A, Bako L, Bhalerao RP. 2011. Short day-mediated cessation of growth requires the downregulation of AINTEGUMENTALIKE1 transcription factor in hybrid aspen. *PLoS Genetics* **7**.

Li ZL, Cui KM. 1988. Differentiation of secondary xylem after girdling. *IAWA Bulletin* **9**: 375–383.

Li ZL, Cui KM, Yu CS, Chang XL. 1981. Anatomical studies of regeneration after ringing of *Eucomma ulmoides*. *Acta Botanica Sinica* **23**: 6–13.

Liu JC, Sheng LH, Xu YQ, Li JQ, Yang ZN, Huang H, Xu L. 2014. *WOX11* and *12* are involved in the first-step cell fate transition during *de novo* root organogenesis in *Arabidopsis*. *Plant Cell* **26**: 1081–1093.

Livak KJ, Schmittgen TD. 2001. Analysis of relative gene expression data using real-time quantitative PCR and the $2^{-\Delta\Delta C_T}$ method. *Methods* **25**: 402–408.

Love J, Bjorklund S, Vahala J, Hertzberg M, Kangasjarvi J, Sundberg B. 2009. Ethylene is an endogenous stimulator of cell division in the cambial meristem of *Populus*. *Proceedings of the National Academy of Sciences, USA* **106**: 5984–5989.

Melnyk CW, Schuster C, Leyser O, Meyerowitz EM. 2015. A developmental framework for graft formation and vascular reconnection in *Arabidopsis thaliana*. *Current Biology* **25**: 1306–1318.

Meng WJ, Cheng ZJ, Sang YL, Zhang MM, Rong XF, Wang ZW, Tang YY, Zhang XS. 2017. Type-B ARABIDOPSIS RESPONSE REGULATORs specify the shoot stem cell niche by dual regulation of *WUSCHEL*. *Plant Cell* **29**: 1357–1372.

Mwange KN, Hou HW, Cui KM. 2003. Relationship between endogenous indole-3-acetic acid and abscisic acid changes and bark recovery in *Eucommia ulmoides* Oliv. after girdling. *Journal of Experimental Botany* **54**: 1899–1907.

Nieminen K, Immanen J, Laxell M, Kauppinen L, Tarkowski P, Dolezal K, Tahtiharju S, Elo A, Decourteix M, Ljung K *et al.* 2008. Cytokinin signaling regulates cambial development in poplar. *Proceedings of the National Academy of Sciences, USA* **105**: 20032–20037.

Nishihama R, Ishizaki K, Hosaka M, Matsuda Y, Kubota A, Kohchi T. 2015. Phytochrome-mediated regulation of cell division and growth during regeneration and sporeling development in the liverwort *Marchantia polymorpha*. *Journal of Plant Research* **128**: 407–421.

Osugi A, Sakakibara H. 2015. Q&A: how do plants respond to cytokinins and what is their importance? *BMC Biology* **13**: e102.

Pang Y, Zhang J, Cao J, Yin SY, He XQ, Cui KM. 2008. Phloem transdifferentiation from immature xylem cells during bark regeneration after girdling in *Eucommia ulmoides* Oliv. *Journal of Experimental Botany* **59**: 1341–1351.

Pernisova M, Klima P, Horak J, Valkova M, Malbeck J, Soucek P, Reichman P, Hoyerova K, Dubova J, Friml J *et al.* 2009. Cytokinins modulate auxin-induced organogenesis in plants via regulation of the auxin efflux. *Proceedings of the National Academy of Sciences, USA* **106**: 3609–3614.

Randall RS, Miyashima S, Blomster T, Zhang J, Elo A, Karlberg A, Immanen J, Nieminen K, Lee JY, Kakimoto T *et al.* 2015. *AINTEGUMENTA* and the D-type cyclin *CYCD3;1* regulate root secondary growth and respond to cytokinins. *Biology Open* **4**: 1229–1236.

Schaller GE, Bishopp A, Kieber JJ. 2015. The yin-yang of hormones: cytokinin and auxin interactions in plant development. *Plant Cell* **27**: 44–63.

Schrader J, Baba K, May ST, Palme K, Bennett M, Bhalerao RP, Sandberg G. 2003. Polar auxin transport in the wood-forming tissues of hybrid aspen is under simultaneous control of developmental and environmental signals. *Proceedings of the National Academy of Sciences, USA* **100**: 10096–10101.

Sena G, Wang XN, Liu HY, Hofhuis H, Birnbaum KD. 2009. Organ regeneration does not require a functional stem cell niche in plants. *Nature* **457**: 1150–1153.

Skoog F, Miller CO. 1957. Chemical regulation of growth and organ formation in plant tissues cultured *in vitro*. *Symposia of the Society for Experimental Biology* **11**: 118–130.

Smetana O, Mäkilä R, Lyu M, Amiryousefi A, Sánchez Rodríguez F, Wu MF, Solé-Gil A, Leal Gavarrón M, Siligato R, Miyashima S *et al.* 2019. High levels of auxin signalling define the stem-cell organizer of the vascular cambium. *Nature* **565**: 485–489.

Spicer R, Tisdale-Orr T, Talavera C. 2013. Auxin-responsive DR5 promoter coupled with transport assays suggest separate but linked routes of auxin transport during woody stem development in *Populus*. *PLoS ONE* **8**: e72499.

Uggla C, Moritz T, Sandberg G, Sundberg B. 1996. Auxin as a positional signal in pattern formation in plants. *Proceedings of the National Academy of Sciences, USA* **93**: 9282–9286.

Vatén A, Dettmer J, Wu S, Stierhof Y, Miyashima S, Yadav RY, Roberts CJ, Campilho A, Bulone V, Lichtenberger R *et al.* 2011. Callose biosynthesis regulates symplastic trafficking during root development. *Developmental Cell* **21**: 1144–1155.

Xie B, Wang XM, Zhu MS, Zhang ZM, Hong ZL. 2011. *CalS7* encodes a callose synthase responsible for callose deposition in the phloem. *The Plant Journal* **65**: 1–14.

Xu L, Huang H. 2014. Genetic and epigenetic controls of plant regeneration. *Mechanism of Regeneration* **108**: 1–33.
Zhang J, Gao G, Chen JJ, Taylor G, Cui KM, He XQ. 2011. Molecular features of secondary vascular tissue regeneration after bark girdling in *Populus*. *New Phytologist* **192**: 869–884.
Zhang J, Nieminen K, Serra JAA, Helariutta Y. 2014. The formation of wood and its control. *Current Opinion in Plant Biology* **17**: 56–63.
Zhao XY, Su YH, Zhang CL, Wang L, Li XG, Zhang XS. 2013. Differences in capacities of *in vitro* organ regeneration between two *Arabidopsis* ecotypes Wassilewskija and Columbia. *Plant Cell Tissue and Organ Culture* **112**: 65–74.

Supporting Information

Additional Supporting Information may be found online in the Supporting Information section at the end of the article.

Fig. S1 The effect of different auxin concentrations on the regeneration of secondary vascular tissue (SVT) after bark girdling in *Populus* wild-type (WT) trees.

Fig. S2 Phylogenetic tree of *APL* genes from *Arabidopsis* and *Populus* homologs.

Fig. S3 Phylogenetic tree of *CALS7* genes from *Arabidopsis* and *Populus* homologs.

Fig. S4 The radical transcriptional expression of *PtAPL-1*, *PtAPL-2*, *PtCALS7-1* and *PtCALS7-2* across the *Populus* wood formation zone.

Fig. S5 Phloem regeneration upon different cytokinin concentrations during *in vitro* secondary vascular tissue regeneration after bark girdling in *Populus*.

Fig. S6 Selection of *PttLMX5::CKI1* transgenic line for secondary vascular tissue regeneration assays.

Table S1 Primer information used for qRT-PCR analysis.

Table S2 *P* values from Student's *t*-test for the expression profiles.

Please note: Wiley Blackwell are not responsible for the content or functionality of any Supporting Information supplied by the authors. Any queries (other than missing material) should be directed to the *New Phytologist* Central Office.